

Ancilla assisted quantum state tomography in multiqubit registers

Abhishek Shukla¹, K. Rama Koteswara Rao², and T. S. Mahesh¹

¹*Department of Physics and NMR Research Center,
Indian Institute of Science Education and Research, Pune 411008, India*

²*Department of Physics and CQIQC, Indian Institute of Science, Bangalore 560012, India*

1 Introduction

Complete characterization of the quantum state is often necessary to optimize the control fields and to understand the effects of environmental noise. In experimental quantum information studies, Quantum State Tomography (QST) is an important tool that is routinely used to characterize an instantaneous quantum state [1]. QST can be performed by a series of measurements of noncommuting observables which together enables one to reconstruct the complete complex density matrix. In the standard method, the required number of independent experiments grows exponentially with the number of input qubits [2,3]. Anil Kumar and co-workers have illustrated QST using a single two-dimensional nuclear magnetic resonance (NMR) spectrum [4]. Later Nieuwenhuizen and co-workers have shown that it is possible to reduce the number of independent experiments in the presence of an ancilla register initialized to a known state [5]. We refer to this method as Ancilla Assisted QST (AAQST). This method was experimentally illustrated by Suter and co-workers using a single input qubit and a single ancilla qubit [6].

Single shot mapping of density matrix by AAQST method not only reduces the experimental time, but also alleviates the need to prepare the target state several times. Often slow variations in system Hamiltonian may result in systematic errors in repeating the state preparation. Further, environmental noises lead to random errors in multiple preparations. These errors play important roles in the quality of the reconstruction of the target state. Therefore AAQST has the potential to provide a more reliable way of tomography.

In this work we first revisit the theory of QST and AAQST and provide methods for explicit construction of the constraint matrices, which will allow extending the tomography procedure for large registers. An important feature of the method described here is that it requires only global rotations and short evolutions under the collective internal Hamiltonian. We also describe NMR demonstrations of AAQST on two different types of systems: (i) a two-qubit input register using a one-qubit ancilla in an isotropic liquid-state system and (ii) a three-qubit input register using a two-qubit ancilla register in a partially oriented system.

2 QST versus AAQST

Consider a general density matrix ρ of an n -qubit system having $N^2 - 1$ unknowns with $N = 2^n$. A single measurement of an observable can only yield a fraction of these unknowns. For example, in NMR, a single measurement of transverse signal can yield nN unknowns. In order to quantify the remaining unknowns, one can measure some other observables, or alternatively, can apply a known unitary U to the initial density matrix and then measure the transverse signal.

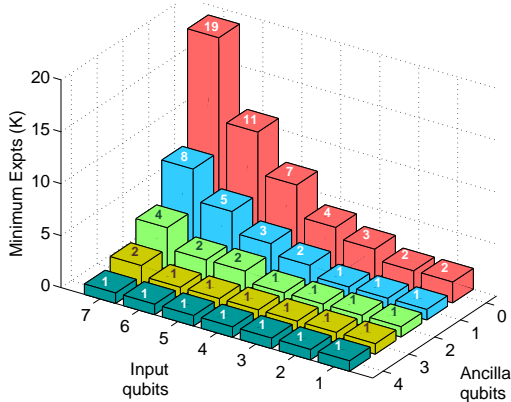


Figure 1: Minimum number of independent experiments required for QST (with zero ancilla) and AAQST.

The minimum number of experiments is $K_{QST} = \left\lceil \frac{N^2-1}{nN} \right\rceil$, where $\lceil \cdot \rceil$ represents the smallest integer larger than the argument. The top array of Fig. 1 illustrates the values of K for different sizes of input register. As anticipated, K increases rapidly as $O(N/n)$ with the number of input qubits.

Suppose the input register of n -qubits is associated with an ancilla register consisting of \hat{n} qubits. The dimension of the combined system of $\tilde{n} = n + \hat{n}$ qubits is $\tilde{N} = N\hat{N}$, where $\hat{N} = 2^{\hat{n}}$. For simplicity we assume that each qubit interacts sufficiently with all other qubits so as to obtain a completely resolved spectrum yielding $\tilde{n}\tilde{N}$ real parameters. Further for simplicity, we assume that the ancilla register begins with the maximally mixed state, so that it does not contribute to the spectral intensities. Thus the deviation density matrix of the combined system is $\tilde{\rho} = \rho \otimes \mathbb{1}_{\hat{N}}/\hat{N}$. We consider applying a non-local unitary exploiting the input-ancilla interaction, We now record the spectrum of the combined system corresponding to the observable $\sum_{j=1}^{\tilde{n}} \sigma_{jx} + i\sigma_{jy}$. Each spectral line can again be expressed in terms of the unknown elements of the ancilla matrix. The spectrum of the combined system yields $\tilde{n}\tilde{N}$ linear equations. The minimum number of independent experiments needed now is $K_{AAQST} = \left\lceil \frac{N^2-1}{\tilde{n}\tilde{N}} \right\rceil$. Compared to K_{QST} , the numerator has not changed since we started with a known state of the ancilla, but the denominator has increased according to the size of the composite system. Since we can choose $\tilde{N} \gg N$, AAQST needs fewer than $O(N/n)$ experiments required in the standard QST. In particular, when $\tilde{n}\tilde{N} \geq (N^2 - 1)$, a single optimized unitary suffices for QST.

3 Experiments

We report experimental demonstrations of AAQST on two spin-systems of different sizes and environments. The experimental result of one of the systems is shown in the following figure. We used three spin-1/2 ^{19}F nuclei of iodotrifluoroethylene (Fig. 2a) dissolved in acetone- D_6 as a 3-qubit system. We have chosen F_1 as the ancilla qubit and F_2 and F_3 as the input qubits. QST was performed for two different density matrices (i) thermal equilibrium state, i.e., $\rho_1 = \frac{1}{2}(\sigma_z^2 + \sigma_z^3)$, and (ii) state after a $(\pi/4)_{\pi/4}$ pulse applied to the thermal equilibrium state, i.e., $\rho_2 = \frac{1}{2}(\sigma_x^2 + \sigma_x^3) - \frac{1}{2}(\sigma_y^2 + \sigma_y^3) + \frac{1}{\sqrt{2}}(\sigma_z^2 + \sigma_z^3)$. The results of the single-shot tomography are displayed in Fig. 2b.

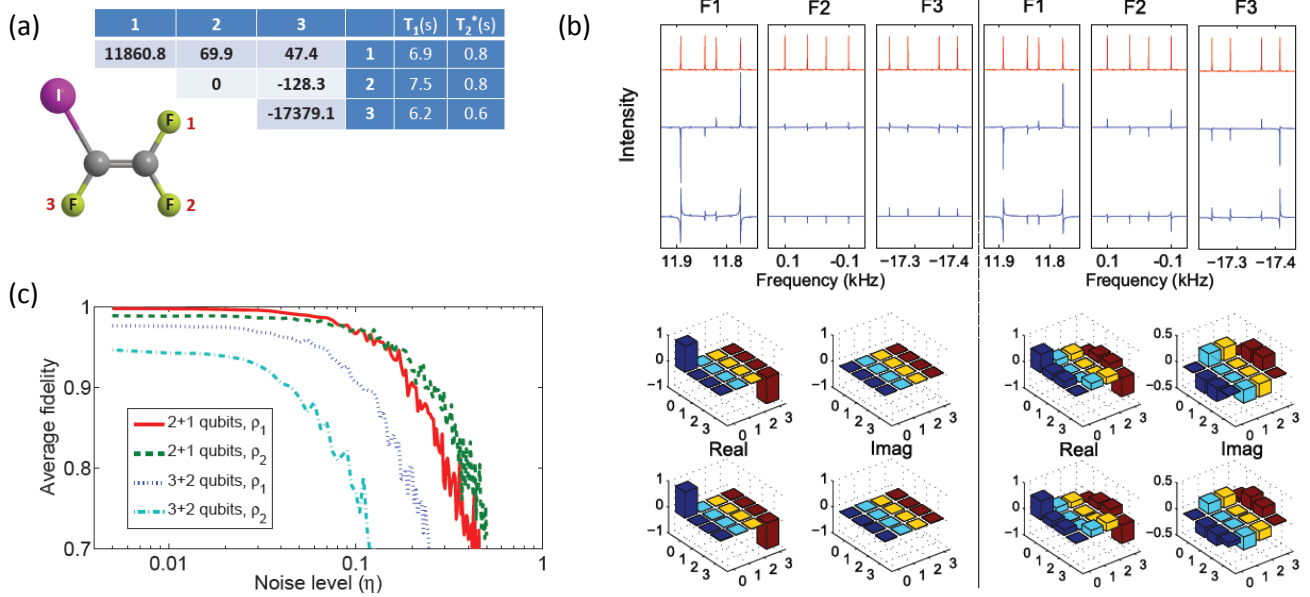


Figure 2: (a) Molecular structure of iodotrifluoroethylene, the table of Hamiltonian parameters and relaxation constants. Chemical shifts and J-coupling constants are shown in Hz. (b) AAQST results for thermal equilibrium state ρ_1 (left column), and that of state ρ_2 (right column), described in the text. The reference spectra is in the top trace. The spectra corresponding to the real part (middle trace) and the imaginary part (bottom trace) of the ^{19}F signal are obtained in a single shot AAQST experiment. The bar plots correspond to theoretically expected states (top row) and those obtained from AAQST experiments (bottom row). Fidelities of the states are 0.997 and 0.99 respectively for the two density matrices. (c) Average fidelity versus noise level.

We now describe the robustness of the AAQST procedure to random noises. In order to study the robustness, we generated a random vector whose elements are in the range $[-\eta, \eta]$ and added it to the experimentally obtained spectral intensities. The resulting profiles of the average fidelity for the two target states ρ_1 and ρ_2 are shown respectively by solid and dashed lines in Fig. 2c. It is evident that the AAQST procedure is very robust in both of these cases, and the average fidelity remained above 0.9 for $\eta < 0.2$.

4 Conclusions

We provided methods for explicit construction of tomography matrices in large registers. We also discussed the optimization of tomography experiments based on minimization of the condition number of the constraint matrix. Further, we demonstrated the experimental ancilla-assisted quantum state tomography in two systems: (i) a system with two input qubits and one ancilla qubit in an isotropic medium and (ii) a system with three input qubits and two ancilla qubits in a partially oriented medium. In both the cases, we successfully reconstructed the target density matrices with a single quadrature detection of transverse magnetization. Finally, we analysed the robustness of the tomography procedure against random noise. We believe that the methods introduced in this work are useful for extending the range of quantum state tomography to larger registers.

References

1. M. A. Nielsen and I. L. Chuang, *Quantum Computation and Quantum Information*, Cambridge University Press (1994).
2. I. L. Chuang, N. Gershenfeld, M. G. Kubinec, and D.W. Leung, *Proc. R. Soc. London. ser A*, 454, 447 (1998).
3. D. Leung, L. Vandersypen, X. Zhou, M. Sherwood, C. Yannoni, M. Kubinec, and I. L. Chuang, *Phys.Rev. A*, 60, 1924 (1999).
4. R. Das, T. S. Mahesh, and A. Kumar, *Phys. Rev. A*, 67, 062304 (2003).
5. A. E. Allahverdyan, R. Balian, and T. M. Nieuwenhuizen, *Phys. Rev. Lett.* 92, 120402 (2004).
6. X. Peng, J. Du, and D. Suter, *Phys. Rev. A*, 76, 42117 (2007).